University of Siena – Department of Medical Biotechnologies

Doctorate in Genetics, Oncology and Clinical Medicine (GenOMeC)

XXXIV cycle (2018-2021)

Coordinator: Prof. Francesca Ariani

MAPK15 Induces Mitophagy and Protects from Oxidative Stress-Dependent Cellular Senescence

Scientific disciplinary sector: MED/03 – Medical Genetics

Tutor

Dr. Mario Chiariello

PhD Candidate

Lorenzo Franci

Firmato digitalmente da FRANCI LORENZO
C = IT

Academic Year 2020/2021

INDEX **Pag.**

ABSTRACT

Mitochondria are the major source of reactive oxygen species (ROS), whose aberrant production by dysfunctional mitochondria leads to oxidative stress, thus contributing to aging as well as to the pathogenesis of various diseases, such as neurodegenerative disorders and cancer. Cells efficiently eliminate damaged mitochondria through a selective type of autophagy, named mitophagy. Here, we unveil the involvement of the atypical MAP kinase family member MAPK15 in mechanisms preserving mitochondrial quality, ultimately affecting DNA damage and senescence. We demonstrate that reduced MAPK15 expression strongly decreases mitochondrial respiration and ATP production, while increasing mitochondrial ROS levels. We show that MAPK15 controls the mitophagic process by recruiting damaged mitochondria to autophagosomal and lysosomal compartments, thus leading to a reduction in the mass of these dysfunctional organelles, but also by participating in the reorganization of the mitochondrial network that usually anticipates their disposal. Ultimately, we demonstrate that mitophagy induction by MAPK15 protects cells from accumulation of nuclear DNA damage due to mitochondrial ROS and, consequently, from senescence deriving from this chronic DNA insult. Altogether, our results indicate a new specific role for MAPK15 in controlling mitochondrial fitness by efficient disposal of old and damaged organelles and suggest this kinase as a potential therapeutic target in diverse human diseases where these processes are deregulated.

Introduction

Besides representing the main source of adenosine tri-phosphate (ATP) synthesis, mitochondria are also crucial in many other cellular processes such as apoptosis, necrosis, autophagy, stress regulation, intermediary metabolism, Ca^{2+} storage and innate immunity [1]. Consequently, their dysfunctions are associated with many human diseases [2]. Importantly, although the electron transport chain (ETC) is very efficient during oxidative phosphorylation (OXPHOS), approximately 1–3% of mitochondrial oxygen consumed during this process is incompletely reduced, with "leaky" electrons quickly interacting with molecular oxygen to form superoxide anions, the predominant reactive oxygen species (ROS) in mitochondria [3]. Therefore, while small amounts of mitochondrial ROS (mt-ROS) are a normal byproduct of OXPHOS, impairment or reduced efficiency in mitochondrial respiration induce an increased level of mt-ROS, which, when not properly eliminated, may become highly toxic for the integrity of the cell [4]. An established consequence of mitochondrial dysfunction is cellular senescence, a complex stress response by which proliferative cells permanently lose the ability to divide. Cell senescence displays a suppressive effect on the development of cancer and other proliferative diseases [5]. However, an excessive senescence can cause or contribute to different aging-associated phenotypes and diseases [6].

In physiological conditions, mitochondria are constantly kept under strict quality control [7]. A marked mitochondrial dysfunction can activate organelle turnover by stimulating its degradation through a selective type of autophagy, a process named mitophagy, demonstrated to occur *in vivo* in many tissues both as a housekeeping, basal mechanism, and upon multiple stressful stimuli, i.e., starvation, high fat diet, ischemia and hypoxia [8]. Mitophagy starts when damaged organelles are recognized by autophagosomes through ubiquitin-dependent or -independent LC3 adapters [9]. Currently, the best studied mitophagy pathway is regulated by the Parkinson's disease (PD) proteins PTEN Induced Kinase 1 (PINK1) and Parkin (PRKN; PARK2) [8]. Specifically, mitochondrial depolarization triggers stabilization and activation of PINK1 resulting in phosphorylation of Ubiquitin at Serine 65, a key signal for PRKN recruitment and activation [8]. Ultimately, PRKN, which is part of a multiprotein E3 ubiquitin ligase complex, conjugates ubiquitin to outer mitochondrial membrane (OMM) proteins, marking these organelles for degradation through the autophagic machinery [10].

A role for the mitogen activated protein kinase 15 (MAPK15; ERK8; ERK7) protein, an atypical member of the MAP kinase family [11], has been recently shown in different mechanisms used by cells to manage stressful stimuli. Starvation, ionizing radiations or chemical insult due to cigarette smoke are all examples of stimuli requiring MAPK15 for mounting a defensive cellular response [11, 12]. Particularly, starvation induces a complex series of events aimed at preserving cell survival under conditions of limited availability of nutrients, with MAPK15 participating in many starvation-dependent cellular events among which Unc-51 Like Autophagy Activating Kinase 1 (ULK1; ATG1)-dependent induction of autophagy [13, 14] and inhibition of protein secretion [15]. DNA damage also starts a complex cellular program aimed at repairing DNA lesions [16] and MAPK15 has been involved in cell mechanisms aimed at coping with different mutagenic sources [17–19], cooperating with proteins deeply involved in DNA repair or maintenance [20, 21]. Very recently, work on chronic obstructive pulmonary disease, a pathology already correlated to mitochondrial dysfunction and mitophagy-dependent necroptosis [22], has suggested a role for MAPK15 in these events [12]. Still, a clear demonstration of MAPK15 involvement in these processes is missing. Importantly, we have already suggested a role for MAPK15 in intracellular pathways potentially able to generate oxidative stress and DNA damage [19]. As mitochondria are the major intracellular source of ROS under normal physiological conditions [23], here we tested the hypothesis that MAPK15 might participate in mechanisms of mitochondrial quality control, namely, mitophagy and, therefore, that its inhibition might contribute to DNA damage and cellular senescence.

Results

Mitochondrial respiration is altered in HeLa cells upon MAPK15 down regulation

Deregulation of homeostatic processes supervising mitochondria integrity and functional efficiency often manifests as alterations in the ability to produce ATP through OXPHOS. Therefore, we decided to evaluate the impact of MAPK15 deregulation on mitochondrial respiratory function, which can be readily examined using the Seahorse metabolic analyzer [24]. Importantly, we decided to use the HeLa cells to perform following experiments, as they do not express the PRKN gene [25], which is often necessary for an efficient mitophagic process [8], allowing us to rescue its expression by transfecting it, when necessary.

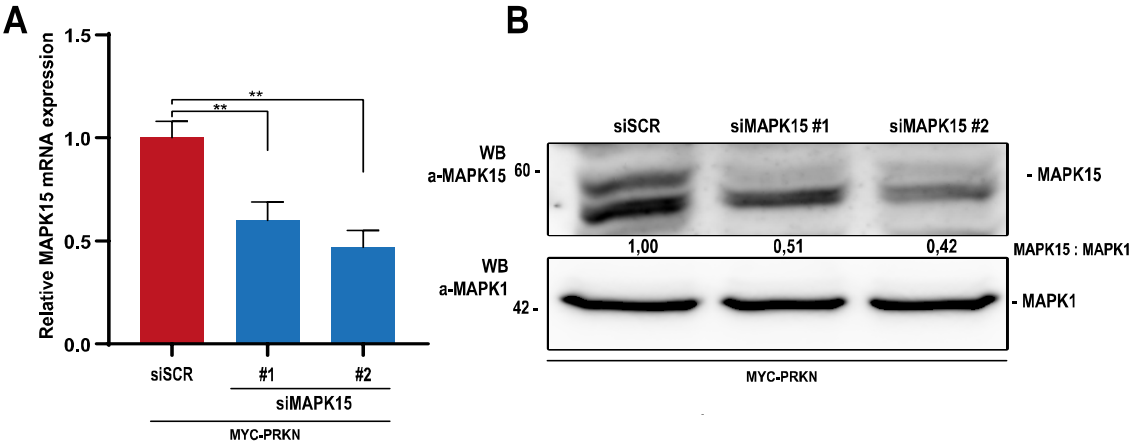

Figure 1. Efficacy of endogenous MAPK15 knockdown by specific siRNA in HeLa cells. HeLa cells were transfected with scrambled siRNA or two different MAPK15 siRNA (#1 or #2) and, after 24 hrs, they were transfected also with MYC-PRKN. Seventy-two hours after siRNA transfection, cells were collected and subjected to qRT-PCR to monitor mRNA expression (**A**) or to western blot analysis for to monitor endogenous MAPK15 protein levels (**B**).

HeLa cells expressing reduced levels of the MAPK15 gene by transient transfection of two specific and unrelated siRNAs (**Fig. 1**) [19, 26] showed a severe decrease of total basal (i.e. in the absence of mitochondrial inhibitors) ATP production, that was mainly due to a reduced ability to generate ATP by OXPHOS (mitoATP) rather than to a decreased glycolytic production of ATP (glycoATP) (**Fig. 2A**). Accordingly, evaluation of Oxygen Consumption Rate (OCR), an established measure of mitochondrial function, showed that basal respiration, an index of energetic demand of the cell under basal conditions, was strongly reduced in cells interfered for MAPK15 expression (**Fig. 2B**). Interestingly, maximal respiration (i.e the maximum rate of respiration that the cell

can achieve) as well as spare respiratory capacity (i.e., an indicator of the capability of the cell to respond to energetic demand) were similarly affected upon MAPK15 knock-down (**Fig. 2B**). Conversely, ExtraCellular Acidification Rates (ECAR), which measures glycolysis, showed a small reduction of glycolysis following MAPK15 interference and no significant differences in glycolytic capacity (i.e., the maximum level of glycolysis that the cell can achieve) nor glycolytic reserve (i.e., an indicator of the capability of the cell to respond to energetic demand) (**Fig. 2C**) [27]. Importantly, effects of MAPK15 deregulation on ATP production was not due to impairment of glucose uptake, as the amount of 2–2-(*N*-(7-Nitrobenz-2-oxa-1,3-diazol-4-yl)Amino)-2-Deoxyglucose (2-NBDG), a fluorescent glucose analogue that can be accumulated inside the cells but cannot be processed [28, 29], was even increased in HeLa cells knocked-down for MAPK15 expression (**Fig. 3**). Overall, our results suggest that MAPK15 affects cellular ATP production primarily by acting on processes controlling homeostasis of the mitochondrial compartment.

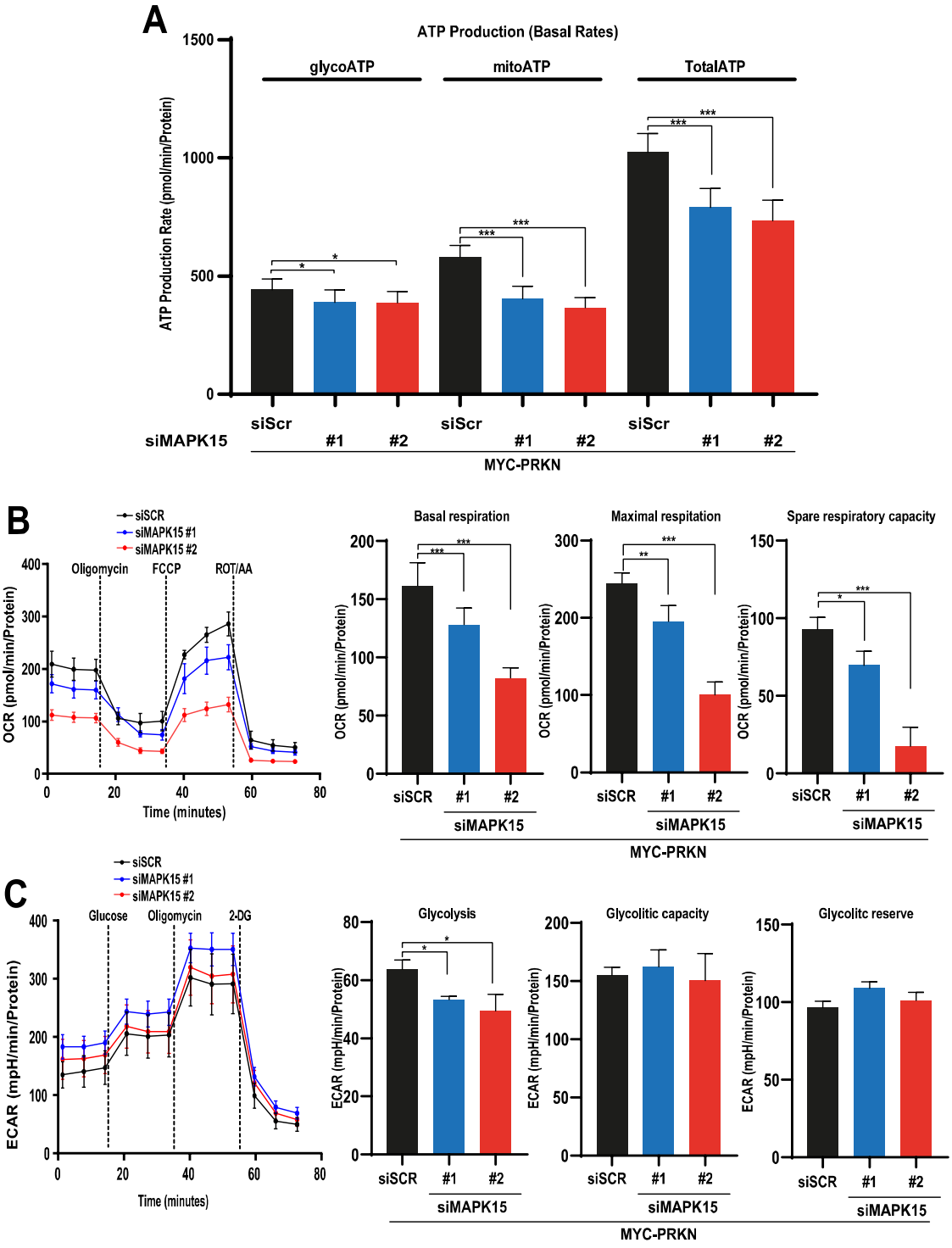

Figure 2. MAPK15 regulates ATP production rates in oxidative phosphorylation and glycolysis. In all experiments, HeLa cells were transfected with scrambled siRNA (negative control) or two different siRNA against MAPK15 (#1 and #2). After 24 hrs, they were also transfected with MYC-PRKN and after additional 48 hrs, we proceeded to analysis through the Seahorse platform. (**A**) Analysis of ATP production. Comparison of mitochondrial ATP (mitoATP) production rate and glycolytic ATP (glycoATP) production rate at basal level. (**B**) Analysis of oxygen consumption rate (OCR) was performed upon subsequent additions of oligomycin, FCCP and the respiratory complex I and III inhibitors rotenone and antimycin A, as indicated. (**C**) Analysis of the extracellular acidification rate (ECAR) with glycolysis stress test. Subsequent additions of glucose, the ATP synthase inhibitor oligomycin, and the hexokinase inhibitor 2-deoxy-glucose (2-DG) were carried out as indicated. One experiment, representative of 3 independent experiments, is shown.

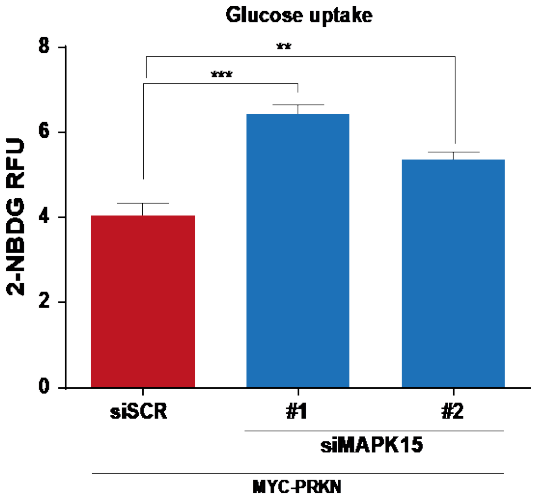

Figure 3. Glucose uptake in MAPK15 knockdown cells. Hela cells were transfected with scrambled siRNA or two different MAPK15 siRNA (#1 or #2) and, after 24 hrs, they were transfected also with MYC-PRKN. Seventy-two hours after siRNA transfection, cells were treated with 2-NDBG (1 hr, 0.02 mg/mL), in FBS- and glucose- free medium, and detected fluorescence with a spectrophotometer. Bars represent the average ± SD Relative fluorescence Unit (RFU) of 2-NDBG fluorescence.

MAPK15 counteracts the formation of mitochondrial Reactive Oxygen Species

Reduced mitochondrial ATP production upon MAPK15 interference suggested us an impairment of mitochondrial respiration, which often determines increased levels of mt-ROS [4]. Therefore, we investigated the impact of MAPK15 deregulation on mt-ROS production. To this aim, we used the fluorogenic dye MitoSOX Red coupled to flow cytometry analysis. Specifically, we measured mt-ROS both in unstimulated conditions and upon two different stimuli known to increase mt-ROS by acting on mitochondrial targets, i.e., rotenone, an inhibitor of mitochondrial complex I [30] and the carbonyl cyanide 4-(trifluoromethoxy) phenylhydrazone (FCCP), a protonophore uncoupler [31]. MAPK15 downregulation by siRNAs, in PRKN-expressing HeLa cells, determined increased levels of mt-ROS as compared to control cells, both in unstimulated conditions (**Fig. 4A-B**) and upon induction of mitochondrial stress by rotenone (**Fig. 4 C-D**) or FCCP (**Fig. 4E-F**), suggesting that MAPK15 functions are important to counteract superoxide production from mitochondria and contribute to their homeostasis. To reinforce these results, we next examined the effects of MAPK15 overexpression on mt-ROS production, in PRKN-expressing unstimulated or rotenone/FCCP-treated HeLa cells. Overexpression of wild-type (WT) MAPK15 determined a reduction of mt-ROS in all conditions tested compared to control (**Fig. 4G-H; Fig. I-L; Fig. 4M-N**), suggesting an increased capacity of these cells to counteract mt-ROS production. Conversely, overexpression of a dominant negative,

kinase dead mutant (MAPK15_KD) [13] induced an increase of mt-ROS levels in all conditions (basal and plus rotenone or FCCP) (**Fig. 4G-H; Fig. 4I-L; Fig. 4M-N**), similarly to the effect of MAPK15 knock-down. Our laboratory has previously described a new LC3-Interacting Region (LIR) motif in MAPK15 and engineered a mutated version of the kinase in this domain, MAPK15_AXXA, which is specifically deficient in its autophagic function [13]. We, therefore, used this mutant to investigate whether the effects of MAPK15 on mitochondrial respiratory function and on mt-ROS production might be ascribed to its ability to affect autophagy [13], possibly regulating the mitophagic process. Indeed, differently from what observed for MAPK15_WT, overexpression of the MAPK15_AXXA mutant was not able to reduce mt-ROS levels in unstimulated (**Fig. 4G-H**), and rotenone- (**Fig. 4I-L**) or FCCP-treated cells (**Fig. 4M-N**). Overall, these data suggest that the autophagic function of this kinase is able to limit mt-ROS superoxide production from mitochondria in basal conditions, e.g., by controlling normal turnover of old organelles, but also to eliminate acutely damaged mitochondria, e.g., upon treatment with agents such as rotenone and FCCP.

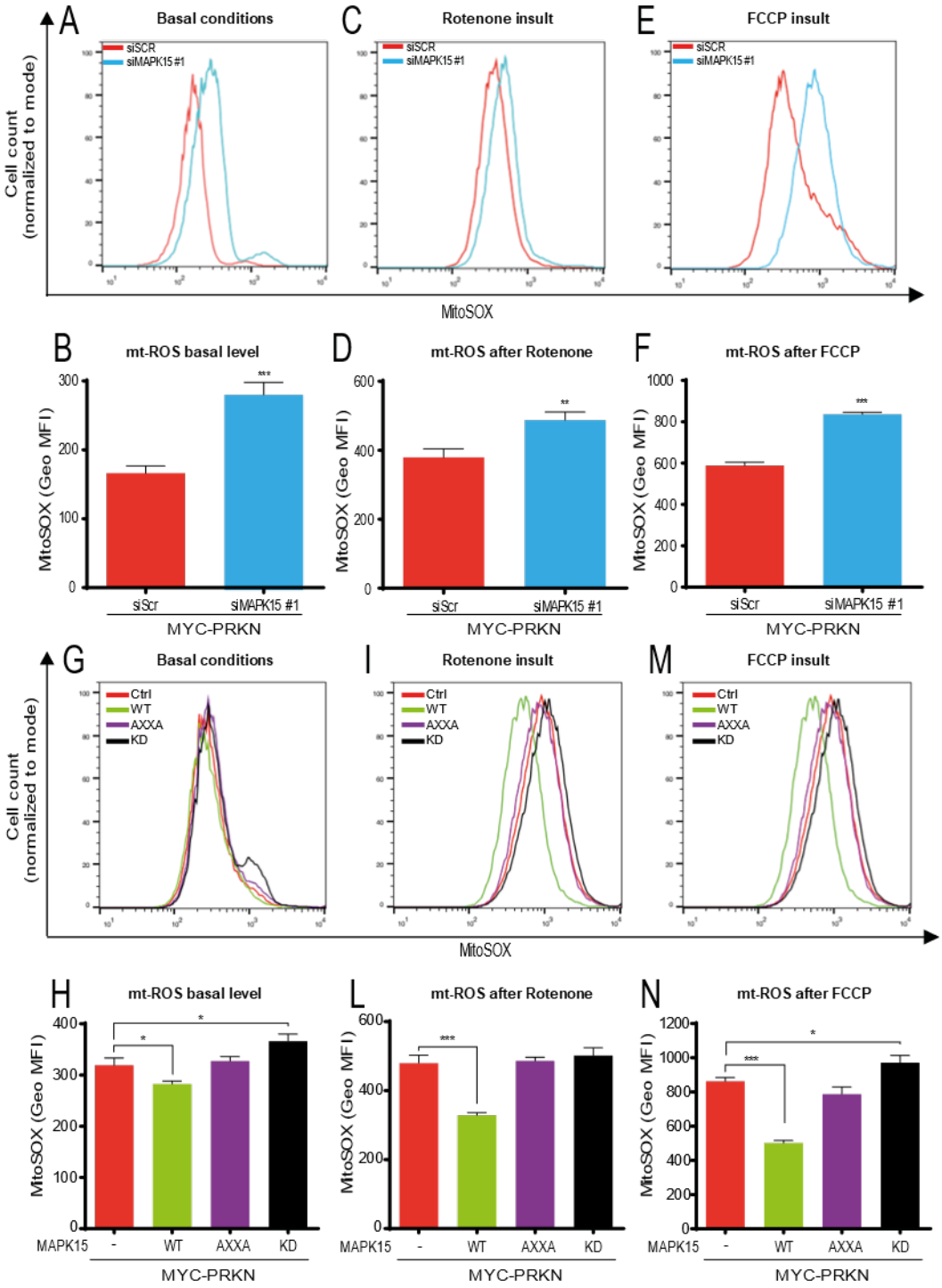

Figure 4. MAPK15 controls production of mt-ROS. (**A, C, E**) Representative FACS histograms or (**B, D, F**) geometric mean fluorescent intensity (GeoMFI) of MitoSOX fluorescence, from HeLa cells transfected with scrambled siRNA (negative control) or MAPK15 siRNA (#1) and, after 24 hrs, also transfected with MYC-PRKN. After additional 48 hrs, samples underwent FACS analysis for MitoSOX red (5μM) fluorescence. Mitochondrial ROS were evaluated in basal conditions (**A**, **B**) and after Rotenone (4 hrs, 5μM) (**C**, **D**), or FCCP (4hrs, 30μM) (**E**, **F**) insults. (**G, I, M**) Representative FACS histograms or corresponding (**H, L, N**) geometric mean fluorescent intensity (GeoMFI) Bars of MitoSOX fluorescence from HeLa cells transiently overexpressing MYC-PRKN and empty vector (Ctrl) or MAPK15 WT or its mutant (AXXA, KD). Twenty-four hours after transfection, samples underwent FACS analysis for MitoSOX red (5μM) fluorescence. Mitochondrial ROS were evaluated in basal conditions (**G, H**) and after Rotenone (4 hrs, 5μM) (**I, L**), or FCCP (4hrs, 30μM) (**M, N**) insults. Bars represents the standard deviation (SD) of 3 independent experiments (n = 3).

MAPK15 increases the fusion of mitochondria with autophagosomal and lysosomal compartments

Currently, there is no clear consensus within the scientific community with regard to a single optimal method for monitoring mitophagy [32]. For this reason, several independent approaches are necessary to support the occurrence of this process [24, 32]. Among them, a key starting point is the demonstration of increased levels of autophagosomes containing or interacting with mitochondria. Therefore, we studied, by confocal microscopy, the effect of MAPK15 overexpression on mitochondria colocalization with puncta marked by LC3B (MAP1LC3B, microtubule-associated protein 1 light chain 3), in unstimulated conditions and after a mitophagic stimulus, i.e., FCCP. Importantly, this approach was coupled to bafilomycin A1 (BAF-A1) treatment, to perform flux analysis [32]. MAPK15 overexpression in PRKN-expressing HeLa cells significantly augmented the number of LC3B puncta colocalizing with mitochondria, both in in basal conditions (full medium) and upon 1-hour FCCP stimulation, and this effect further increased upon BAF-A1 treatment, indicating a positive mitophagic flux (**Fig. 5**).

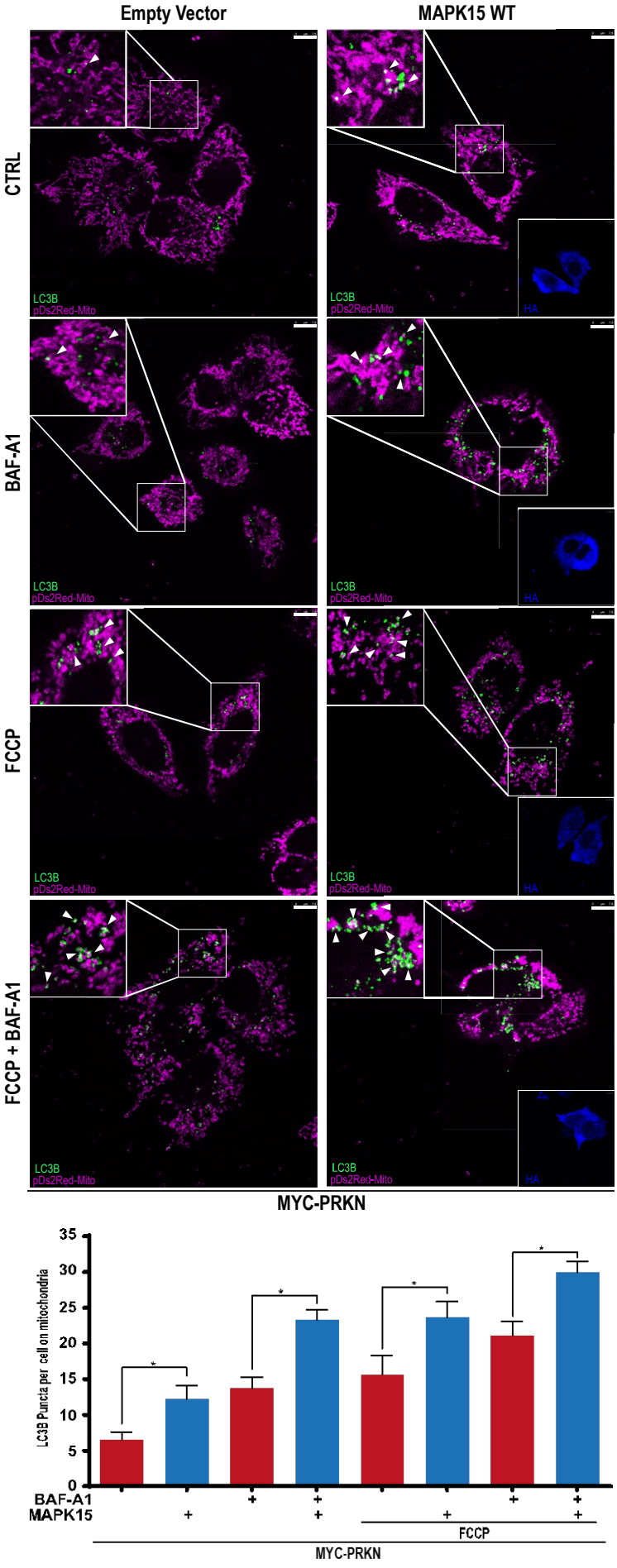

Figure 5. MAPK15 controls internalization of mitochondria into autophagosomes and lysosomes. (**A**) HeLa cells stably expressing pDsRed2-Mito were transfected with MYC-PRKN and empty vector (Ctrl) or HA-MAPK15 WT. After 24 hrs, cells were treated 1 hour with vehicle or 30 μM FCCP or with 100 nM BAF-A1 or 30 μM FCCP plus 100 nM BAF-A1. Cells were next fixed and subjected to immunofluorescence analysis. In these representative images, LC3B is visualized in green and DsRed-Mito in magenta. LC3B dots per cell on mitochondria were also plotted on the accompanying graph as result of five representative fields. Bars represents the SD of 3 independent experiments (n = 3).

To complete the imaging analysis of the mitophagic flux, we next evaluated the fusion process of mitophagosomes with hydrolase-containing lysosomes, which represents the last step in the degradation process along the autophagic route [32]. Again, we chose to study the effect induced by MAPK15 overexpression on the fusion of mitochondria with LAMP1-marked lysosomes. Specifically, we counted the number of mitochondria colocalized with and engulfed in lysosomes [33–35], in PRKN-expressing HeLa cells, and demonstrated that MAPK15 increased the localization of mitochondrial structures inside the lysosomal vesicles both in basal conditions and after the FCCP mitophagic stimulus (**Fig. 6**).

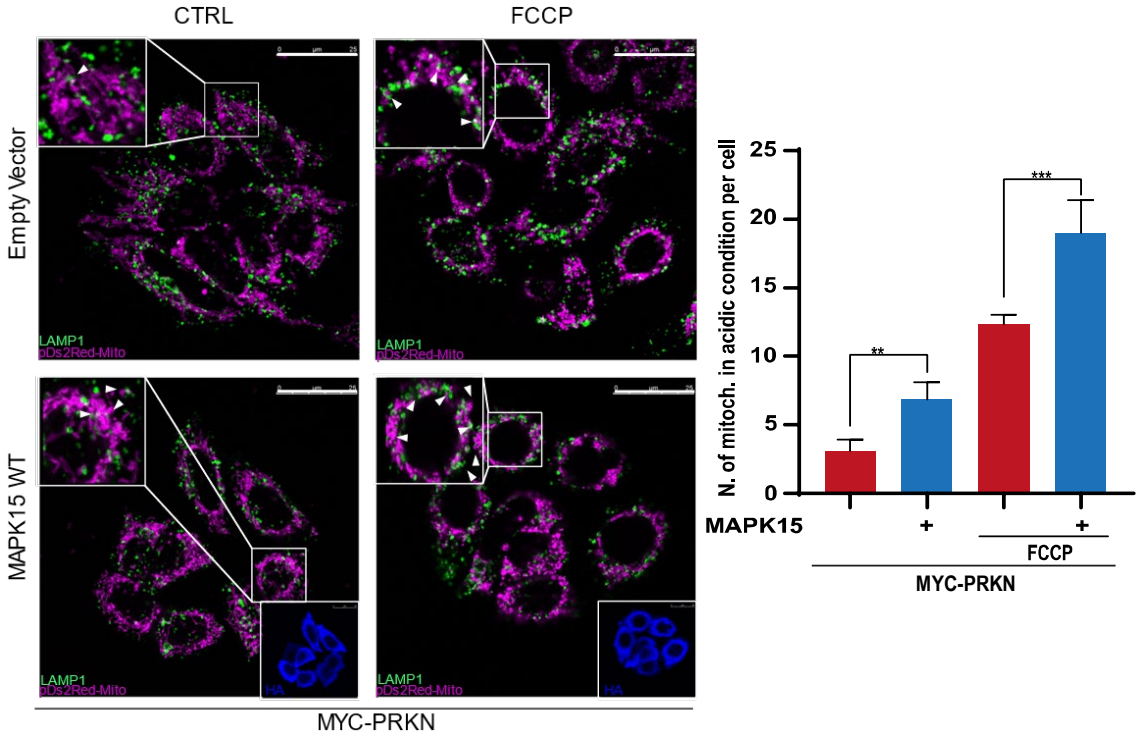

Figure 6. MAPK15 controls internalization of mitochondria into lysosomes HeLa cells stably expressing pDsRed2-Mito were transfected with MYC-PRKN and empty vector (Ctrl) or HA-MAPK15 WT. After 24 hrs, cells were treated 1 hour with vehicle or 30 μM FCCP. Cells were next fixed and subjected to immunofluorescence analysis. In these representative images, LAMP1 is visualized in green and DsRed-Mito in magenta. Number of mitochondria in acidic condition (white) were plotted on the accompanying graph, as result of five representative fields. Bars represents the SD of 3 independent experiments (n = 3).

Overall, these experiments demonstrated the ability of MAPK15 to increase the localization of damaged mitochondria to autophagosomes and, next, to lysosomes, the two vescicular compartments involved in the mitophagic process. Induction of mitophagy can also be monitored by studying recognition of mitochondria by autophagosomes, detecting the enrichment of the LC3B protein in the mitochondrial

fraction by immunoblot analysis [32]. To this aim, we used PRKN-expressing HeLa cells stably overexpressing MAPK15. In line with the hypothesis of a role for MAPK15 in the mitophagic process, we observed an increased amount of LC3B-II in the mitochondrial fraction, (**Fig. 7A**), demonstrating increased recruitment of autophagosomes to mitochondria, a key event in the initiation of mitochondrial disposal through mitophagy [25, 36]. Interestingly, MAPK15 was also present in the mitochondrial fraction (**Fig. 7A**), a localization possibly mediated by protein-protein interactions, since specific mitochondrial targeting sequences are absent in this MAP kinase (e.g., http://busca.biocomp.unibo.it/deepmito/). To establish a functional role for MAPK15 in the mitophagic process by this approach, we also took advantage of HeLa cells stably overexpressing mutated forms of MAPK15, including above-mentioned mutants lacking kinase (MAPK15_KD) or autophagic (MAPK15_AXXA) activities. Interestingly, mitochondrial fractions showed increased of LC3B-II amount in cells expressing the wild-type protein (WT) while displayed a reduction of its levels in those expressing kinase- and autophagy-deficient mutants, both in basal conditions and upon stimulation with the mitophagy inducer FCCP (**Fig. 7B**). These data, therefore, establish a clear dependency of the initial phases of the mitophagic process on the correct functioning of the MAPK15 protein.

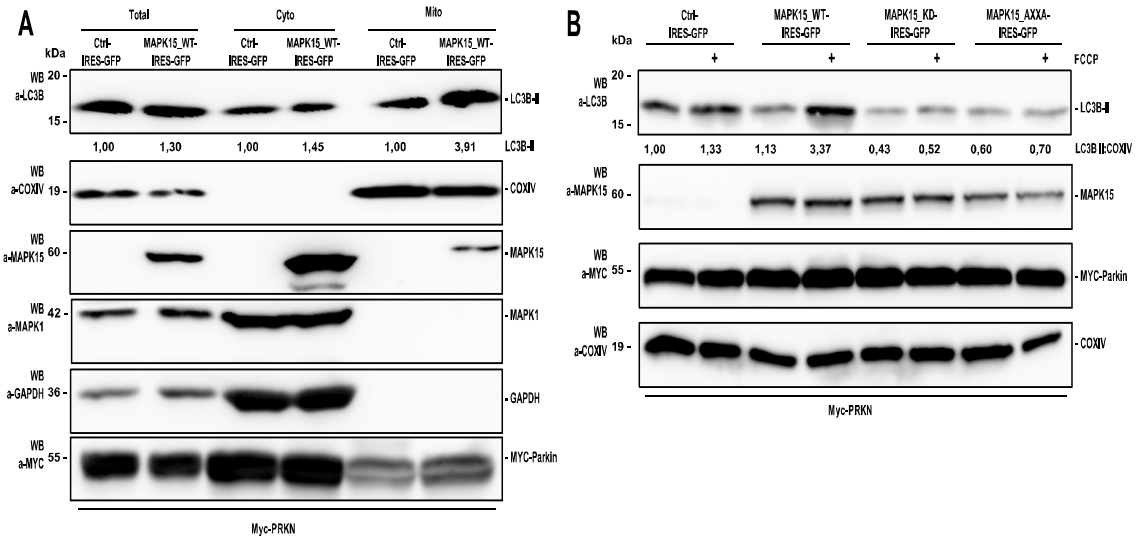

Figure 7. MAPK15 increases LC3B protein levels in mitochondrial-enriched fraction. (**A**) HeLa cells stably expressing the empty vector (Ctrl) or MAPK15_WT were transfected with MYC-PRKN and, after 24 hrs, were subjected to fractioning obtaining mitochondrial enrichment. Lysates were next subjected to SDS-PAGE followed by WB and analysed for indicated proteins. Total, total lysate; Cyto, cytoplasmic fraction; Mito, mitochondrial enrichment. One experiment, representative of 3 independent experiments is shown (n = 3). Densitometric analysis of bands was also performed. (**B**) HeLa cells stably expressing the empty vector (Ctrl), MAPK15_WT, MAPK15_AXXA or MAPK15_KD were transfected with MYC-PRKN and, after 24 hrs, were treated with 30 μM FCCP (1 hr), where indicated, and then subjected to fractioning obtaining mitochondrial enrichment. Lysates were subjected to SDS-PAGE followed by WB for analysis for indicated proteins. One experiment, representative of 3 independent experiments is shown. Densitometric analysis of bands was also performed.

MAPK15 controls mass and dynamics of the mitochondrial compartment

A key step for monitoring mitophagy is the analysis of the mitochondrial mass, to establish the efficiency of the process in eliminating dysfunctional organelles, aged or damaged by toxic substances [32]. We, therefore, decided to evaluate, by western blot analysis, the levels of different mitochondrial proteins, whose changes are directly related to variations of mitochondrial mass, which can be consistently reduced by uncoupling agents such as FCCP [37, 38]. Indeed, TOMM20 (translocase of outer mitochondrial membrane 20) amounts were readily reduced upon FCCP treatment of PRKN-expressing HeLa cells, while its levels increased further upon the same stimulus in cells that were not rescued for PRKN expression (**Fig. 8A)**, compare first and second lane to third and fourth, respectively). This result confirmed that, in our system, FCCP induced PRKN-dependent mitophagic reduction of TOMM20 amounts, which therefore represented a good surrogate for mitochondrial mass. In this system, we transfected MAPK15_WT and its mutated counterparts, MAPK15_KD and MAPK15_AXXA, and demonstrated that the WT protein increased the efficiency in the elimination of mitochondria damaged by FCCP, as demonstrated by a reduction of TOMM20 protein

levels, while both mutants failed to do so, the autophagy-deficient mutant even increasing TOMM20 amounts (**Fig 8A**). Down-regulation of endogenous MAPK15 determined an increase of TOMM20 protein levels in PRKN-expressing cells, in both FCCP-stimulated and -unstimulated conditions (**Fig. 8B**). During mitophagy mediated by PRKN, this protein ubiquitinates a wide range of OMM components, including VDAC1, MFN1/2 and TOMM20, inducing their degradation by the proteasome [32, 39]. Estimating the amount of mitochondrial mass by using a single protein such as TOMM20 may, therefore, be deceiving [40]. Consequently, we decided to monitor four additional mitochondrial proteins with the same methodological approach, upon FCCP treatment, i.e., ATP5A, UQCRC2, SDHB and NDUFB8, part of respiratory chain complexes V, III, II and I, respectively [41]. We confirmed an accumulation of damaged mitochondria due to the lack of functional MAPK15 especially, in FCCP-treated samples, as demonstrated by increased levels of each of these proteins (**Fig. 8C**).

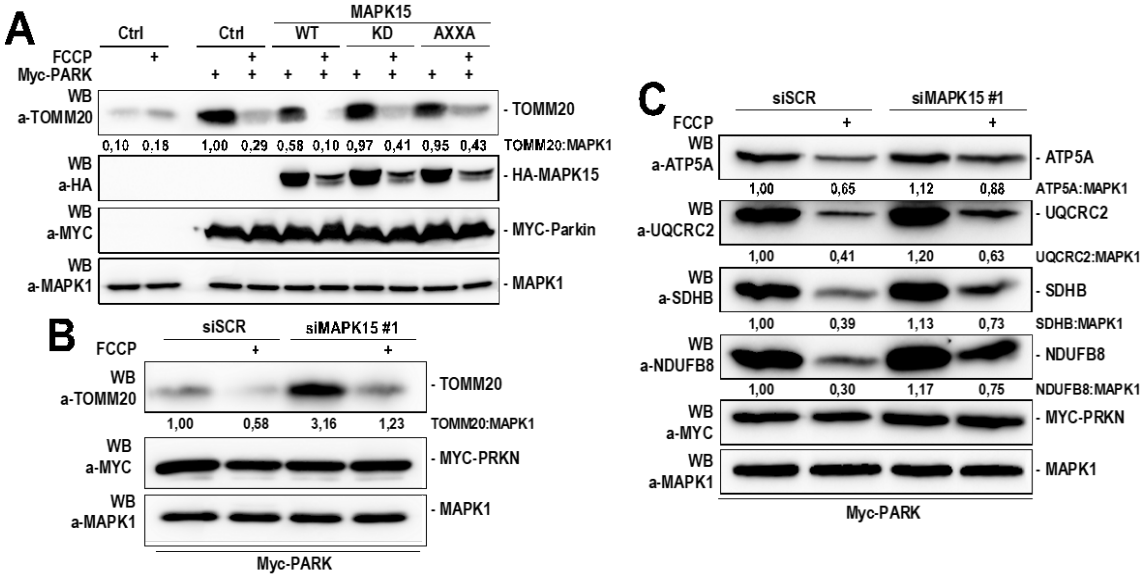

Figure 8. MAPK15 enhances elimination of damaged mitochondria, with consequent decrease of their mass. (**A**) HeLa cells were transfected with MYC-PRKN and the empty vector (Ctrl) or MAPK15_WT or MAPK15_AXXA or MAPK15_KD. After 24 hrs, cells were treated with 30 μM FCCP or vehicle (8 hrs). Lysates were subjected to SDS-PAGE followed by WB and analysed for indicated proteins. First two lanes do not express MYC-PRKN while all other samples express this E3 ubiquitin ligase. (**B**) HeLa cells were transfected with scrambled siRNA or MAPK15 siRNA (#1) and after 24h, were transfected with MYC-PRKN. After additional 48 hrs, samples were treated with 30 μM FCCP or vehicle (8 hrs). Lysates were then subjected to SDS-PAGE followed by WB and analysed for indicated proteins. (**D**) Same as in (**C**) but analysing different proteins. In each case, one experiment, representative of 3 independent experiments is shown. Densitometric analysis of bands was also performed, as indicated.

Quantitative PCR (qPCR) of specific mitochondrial genes may give a reliable estimation of mitochondrial-DNA (mt-DNA) copy number per cell and can be a useful alternative method to estimate mitochondrial mass [32]. We, therefore, overexpressed MAPK15 and its mutated counterparts (KD and AXXA) in PRKN-expressing HeLa cells, stimulated with FCCP, and next quantified mt-DNA copy number by performing qPCR on two mitochondrial genes, MT-ND1 (mitochondrially encoded NADH dehydrogenase1) and MT-ND2, to estimate mitochondrial mass [32]. In these conditions, FCCP reduced the quantity of these two genes and MAPK15_WT cooperated with this stimulus to further decrease their amounts (**Fig. 9A** and **9B**). Conversely, upon FCCP treatment, MAPK15_AXXA could not affect mt-DNA amount while MAPK15_KD even increased it (**Fig. 9A** and **9B**), confirming a role for MAPK15 and its pro-autophagic function in controlling mitophagy, upon mitochondrial damage. Ultimately, to confirm these results in a MAPK15-endogenous setting, we also downregulated its levels by two specific and unrelated siRNA and demonstrated that reduced amounts of this MAP kinase strongly interfered with FCCP on the amounts of mt-DNA (for both MT-ND1 and MT-ND2 genes) (**Fig. 9C** and **9D**) and, consequently, with the efficacy of the mitophagic process induced by the protonophore uncoupler in these cells.

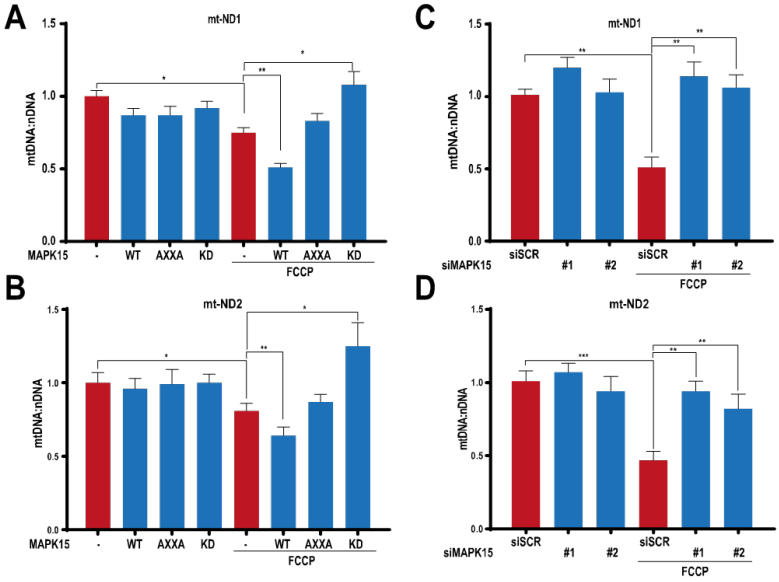

Figure 9. MAPK15 controls mt-DNA elimination after mitophagic stimuli. (**A**) HeLa cells transiently overexpressing MYC-PRKN and empty vector (Ctrl) or MAPK15_WT or MAPK15_AXXA or MAPK15_KD. Twenty-four hours after transfection, samples were treated with 30 µM FCCP or vehicle (8 hrs). DNA was purified using QIAamp DNA Mini Kit and then 10 ng of each sample were subjected to qRT-PCR for mitochondrially encoded NADH dehydrogenase 1 (MT-ND1). The amount of PKM (pyruvate kinase M1/2), a nuclear-encoded gene, was also quantified by qPCR and used for normalization purposes [32] (**B**) Same as in (**A**), but MT-ND2 levels were measured. (**C**) HeLa cells were transfected with scrambled siRNA or two MAPK15 siRNA (#1 or #2) and after 24h, transfected with MYC-PRKN. After additional 48 hrs, samples were treated with 30 µM FCCP or vehicle (8 hrs). DNA was next purified using QIAamp DNA Mini Kit, and then 10 ng of each sample were subjected a qRT-PCR for MT-ND1. The amount of PKM was also quantified by qPCR and used for normalization purposes (**D**) Same as in (**C**), but MT-ND2 levels were measured. Bars represents average ratio ± SD between mitochondrial DNA and nuclear DNA (mtDNA:nDNA). In each case, bars represent the SD of 3 independent experiments (n = 3).

Confocal fluorescence microscopy is another powerful approach that can be used to score the amount of specific mitochondrial markers, to estimate the mass of these organelles [32]. In addition, this approach also allows to get morphological information, which are becoming increasingly important to understand the regulation of homeostatic processes controlling the functions of mitochondria. Based on our data supporting the use of TOMM20 as a reliable endogenous surrogate for estimating mitochondrial mass (see above, **figure 7A**), we visualized mitochondria by anti-TOMM20 antibodies, in PRKN-expressing HeLa cells transfected with bicistronic plasmids expressing green fluorescent protein (GFP) together with wild-type (WT) and mutated forms (KD and AXXA) of MAPK15 [26]. Specifically, in this experiment, we measured the mean volume of mitochondria per cell and showed that MAPK15_WT increased the efficacy of mitophagy after FCCP insult, as demonstrated by a reduction of mitochondrial volume compared to unstimulated cells (**Fig. 10A-B**). Conversely, upon FCCP insult, both MAPK15_KD and MAPK15_AXXA determined an increase of mitochondrial volume (**Fig. 10A-B**), demonstrating reduced capability of autophagy-deficient MAPK15 mutants to support removal of damaged mitochondria. Interestingly, several authors have reported the observation of PRKN-dependent mitochondrial clustering (sometimes called "mito-aggresomes"), often in the perinuclear area, as a consequence of their loss of membrane potential ($\Delta\Psi_m$), upon treatment with uncoupler drugs, such reorganization of the network usually anticipating their lysosomal degradation [25, 42, 43]. Indeed, we also noticed very pronounced perinuclear clusters of mitochondria, in PRKN expressing cells, upon prolonged (> 2 hrs) exposure to FCCP, which were strongly prevented by co-expression of both MAPK15_AXXA and MAPK15_KD mutants (**Fig. 10A**), suggesting a specific role for this MAP kinase in microtubule-dependent dynamics involved in mitophagy [43]. Ultimately, we decided to prove, also in these settings, that endogenous MAPK15 was able to control autophagic disposal of damaged mitochondria. We, therefore, downregulated MAPK15 by a specific siRNA in PRKN-expressing HeLa cells and stimulated them with FCCP, to damage the mitochondrial compartment. As shown in **figure 10C-D**, downregulation of MAPK15 expression prevented the ability of FCCP-treated cells to eliminate mitochondria, which, on the contrary, was very efficient in cells expressing the endogenous MAP kinase. Strikingly, while mitochondria, upon FCCP treatment, changed their appearance from being primarily tubular and organized in an interconnected network throughout the cell body to clusters mostly in the perinuclear area [43], the same treatment barely

affected the morphology and localization of these organelles in cells knockdown for endogenous MAPK15 expression (**Fig. 10C**). Overall, our different approaches therefore clearly demonstrate that MAPK15 is necessary for efficient disposal of damaged mitochondria in mammalian cells, but also suggest a new role for this MAPK15 in microtubule-dependent mitochondrial dynamics.

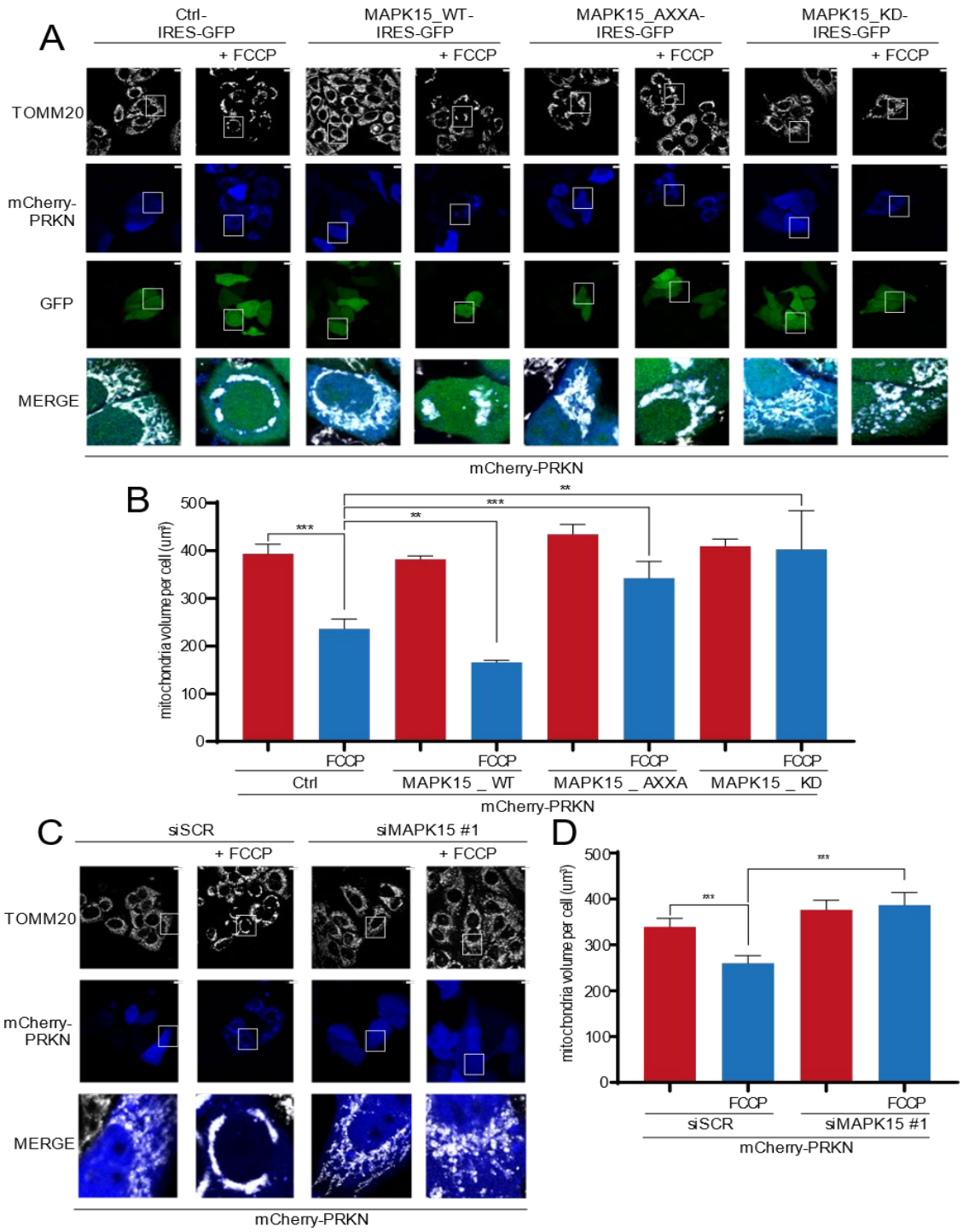

Figure 10. MAPK15 regulates mitochondrial volume and dynamics upon mitophagic stimuli. (**A**) HeLa cells were transfected with mCherry-PRKN and Ctrl-IRES-GFP or MAPK15_WT-IRES-GFP or MAPK15_AXXA-IRES-GFP or MAPK15_KD-IRES-GFP. After 24 h, cells were incubated with 30 μM FCCP or vehicle (4 hrs). Cells were next fixed and subjected to immunofluorescence analysis. In these representative images, TOMM20 is visualized in white, mCherry-PRKN in blue and GFP in green. Scale bars correspond to 10 μm. (**B**) Mitochondria mean volume per cell, expressed in μm^3, was plotted on the accompanying graph. (**C**) HeLa cells were transfected with scrambled siRNA (negative control) or MAPK15 siRNA (#1) and, after 24 hrs, further transfected with plasmid encoding for mCherry-PRKN. After additional 48 hrs, cells were incubated 30 μM FCCP or vehicle (4 hrs). Cells were next fixed and subjected to immunofluorescence analysis. In these representative images, TOMM20 is visualized in white and mCherry-PRKN in blue. Scale bars correspond to 10 μm. (**D**) Mitochondria mean volume per cell, expressed in μm^3, was plotted on the accompanying graph. Bars represents the SD of 3 independent experiments (n = 3).

MAPK15 prevents cellular senescence by protecting genomic integrity from mt-ROS produced by damaged mitochondria

Reduced efficacy in mitochondrial respiration increases generation of mt-ROS which, in turn, damage several cellular components, including nuclear DNA, possibly contributing to senescence but also genomic instability and cancer [16]. Based on the ability of MAPK15 to control mitophagy, we next asked whether ROS specifically generated from mitochondria, as a consequence of decreased fitness, could be responsible for damaging nuclear DNA. To answer this question, we took advantage of a specific mitochondria-targeted antioxidant, mito-TEMPO [44, 45] to interfere with DNA damage induced by down-regulation of MAPK15, in our cellular system. Indeed, mito-TEMPO completely abolished DNA-damage induced by MAPK15 knock-down, in PRKN-expressing HeLa cells (**Fig. 11A-B**), demonstrating that the increase in the production of mt-ROS, due to impaired mitophagy, is the cause of this event so deleterious for the cell.

Cellular senescence is an irreversible growth arrest of damaged or ageing cells and the ability of mitochondria to generate ROS has been clearly linked to this phenotype, by inducing or stabilizing the DNA damage response (DDR) [46, 47]. Indeed, altered mitophagy, and consequent increase of mt-ROS, induces senescence [48]. Therefore, in light of current data, we tested if MAPK15 downregulation could actually induce cellular senescence. Indeed, two specific and non-correlated siRNAs for MAPK15 strongly increased β-galactosidase activity (**Fig. 11C**), a key marker identifying senescent cells [49], supporting a role for MAPK15 in preserving proliferative potential of mammalian cells by maintaining the correct and efficient disposal of old and damaged mitochondria.

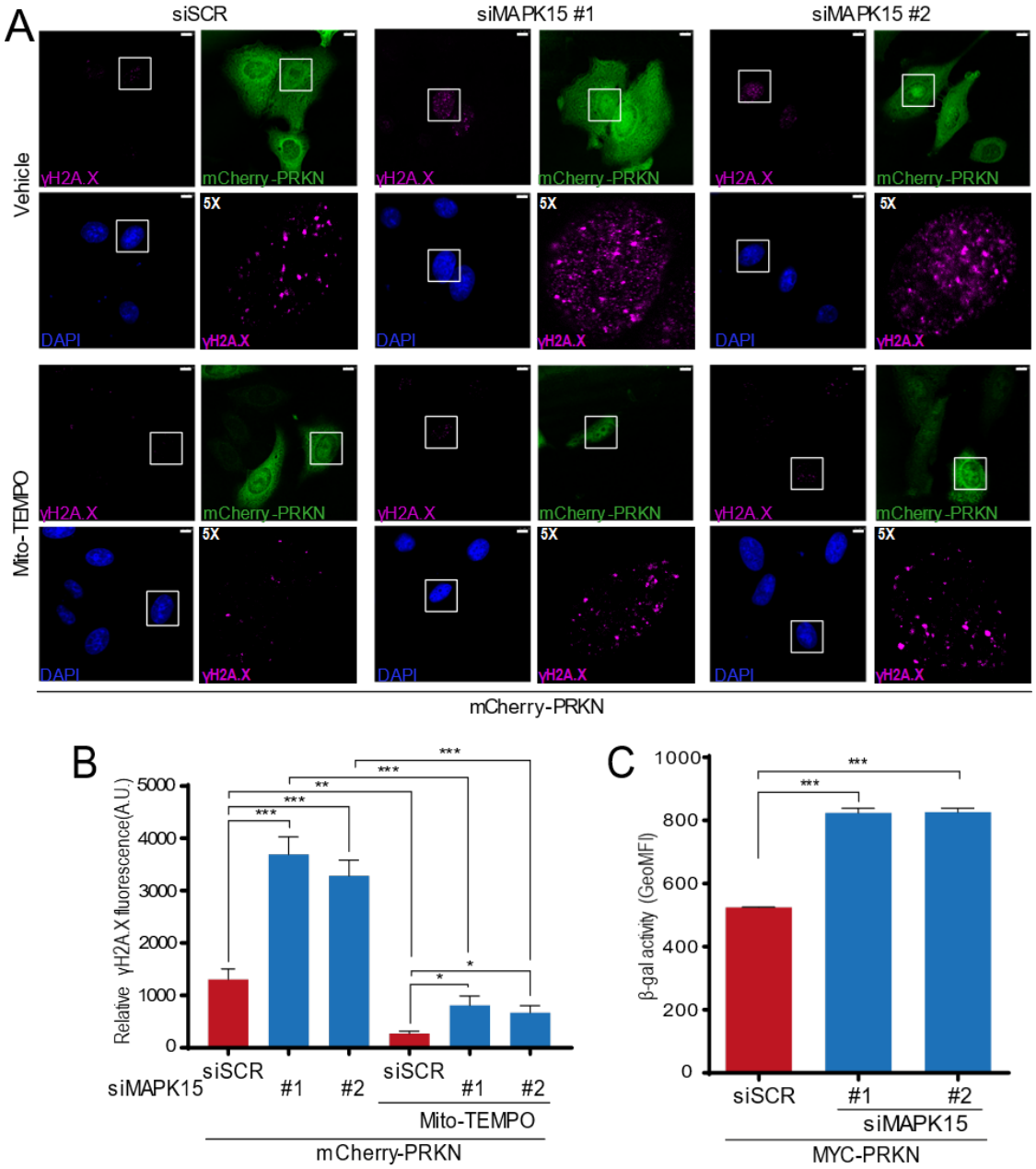

Figure 11. MAPK15 prevents DNA damage induced by mt-ROS and controls cellular senescence in HeLa cells. (**A**) HeLa cells were transfected with scrambled siRNA or two different MAPK15 siRNA (#1 or #2). After 24h, they were transfected with mCherry-PRKN. After additional 24 hrs, cells were treated with 100 μM mito-TEMPO or vehicle (24 hrs). Cells were next fixed and subjected to immunofluorescence analysis. In these representative images, γH2A.X is visualized in magenta, mCherry-PRKN in green and nuclei in blue (DAPI). Scale bars correspond to 7,5 μm. (**B**) Intensitometric analysis of nuclear γH2A.X fluorescence of five representative microscopy fields. (**C**) HeLa cells were transfected with scrambled siRNA or two different MAPK15 siRNA (#1 or #2) and after 24 hrs, they were transfected also with MYC-PRKN. After additional 48 hrs, cells were fixed and incubated with a probe staining senescent cells (β-galactosidase activity). Then, they were analysed by FACS. Bars represents the SD of 3 independent experiments (n = 3).

MAPK15 counteracts formation of mt-ROS, preventing cellular senescence and consequent reduction of proliferative potential, in neuronal SH-SY5Y cells

Although the exact causes contributing to PD pathogenesis are largely unknown, mitochondrial oxidative stress and accumulated dysfunctional mitochondria are critical factors in the onset of the disease [50]. To suggest a potential therapeutic application of our study and confirm biological consequences of our data also in a different cellular system, we next investigated the consequences of MAPK15 down-regulation on mt-ROS-dependent DNA damage, induction of senescence and consequent reduction of cell proliferation in SH-SY5Y cells. This neuroblastoma cell line is, indeed, widely used in PD research [51] and, notably, expresses endogenous PRKN [52].

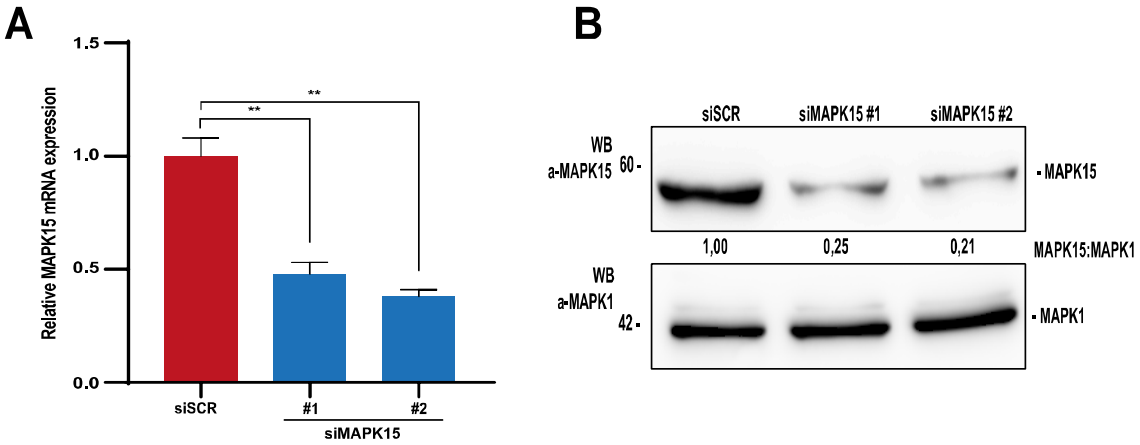

Figure 12. Efficacy of endogenous MAPK15 knockdown by specific siRNA in SH-SY5Y cells. SH-SY5Y cells were transfected with scrambled siRNA or two different MAPK15 siRNA (#1 or #2). Seventy-two hours after siRNA transfection, cells were collected and subjected to qRT-PCR to monitor mRNA expression (**A**) or to western blot analysis for to monitor endogenous MAPK15 protein levels (**B**).

In these neuronal cells, down-regulation of MAPK15 (**Fig. 12**) increased nuclear DNA damage in a mt-ROS dependent manner (**Fig. 13A**), confirming the role of this kinase in the mechanism controlling accumulation of dysfunctional mitochondria. Consequently, MAPK15 knock-down cells also revealed reduced proliferative potential (**Fig. 13B**) and increased β-galactosidase activity (**Fig. 13C**), two key markers of cellular senescence, which could be significantly rescued by treating the cells with mito-TEMPO. These results ultimately indicate that MAPK15 is able to confer protection from oxidative stress-dependent cellular senescence and, possibly, neurotoxicity, thanks to its mitophagic function.

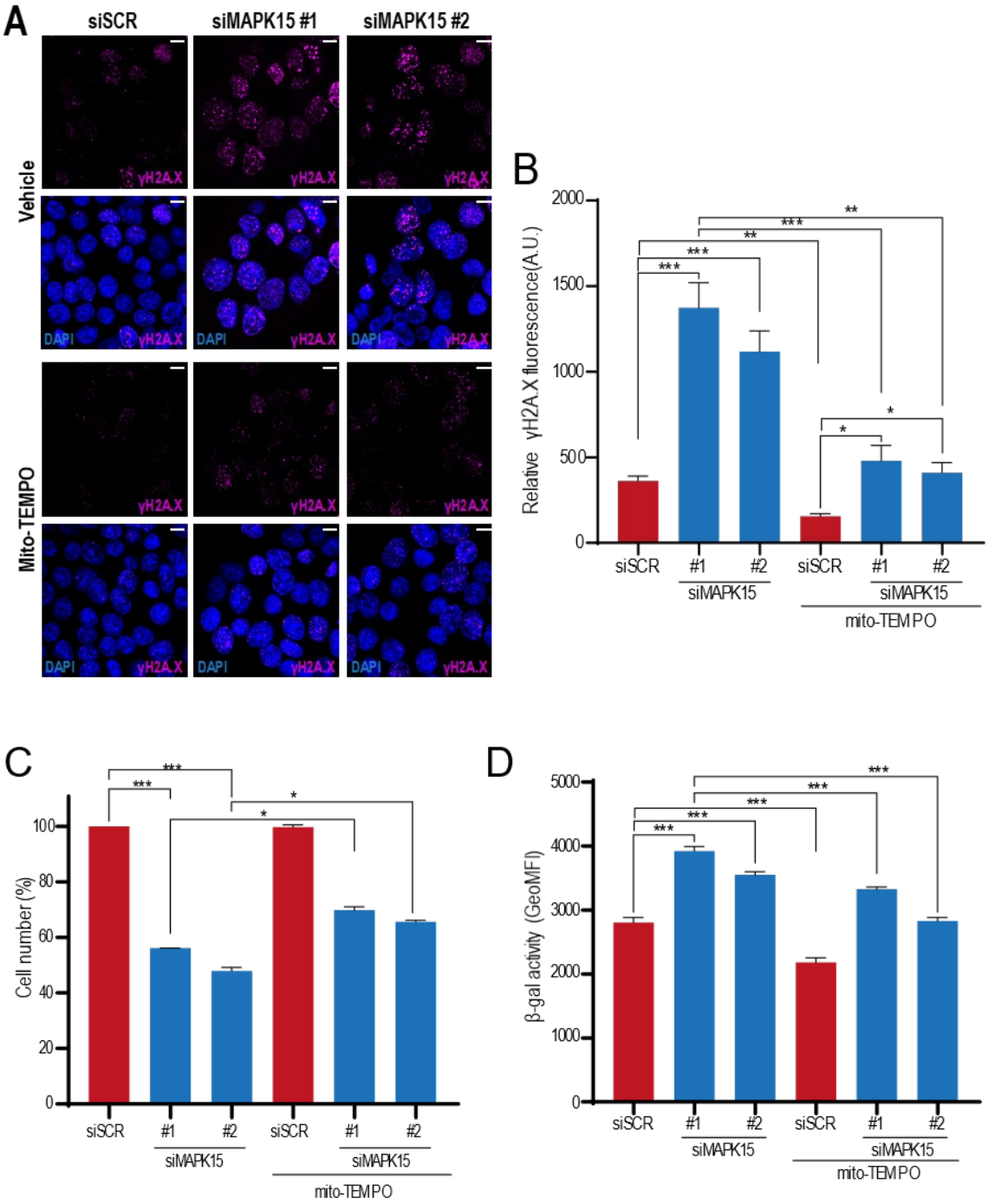

Figure 13. MAPK15 prevents DNA damage and cellular senescence induced by mt-ROS, in neuronal SH-SY5Y cells. (**A**) SH-SY5Y cells were transfected with scrambled siRNA or two different MAPK15-specific siRNA (#1 or #2). After 48 hrs, cells were treated with 100 μM mito-TEMPO or vehicle (24 hrs). Cells were next fixed and subjected to immunofluorescence analysis. In these representative images, γH2A.X is visualized in red and nuclei in blue (DAPI). Scale bars correspond to 10 μm. Intensitometric analysis of nuclear γH2A.X fluorescence from five representative microscopy fields were also plotted on the accompanying graph. (**B**) SH-SY5Y cells were transfected with scrambled siRNA or two different MAPK15 siRNA (#1 or #2) and after 48 hrs, they were treated with 100 μM mito-TEMPO or vehicle (24 hrs). After 72 hrs of transfection, cells were harvested and cell number was evaluated with Z2 Coulter Counter (Beckman Coulter) (**C**) SH-SY5Y cells were transfected with scrambled siRNA or two different MAPK15 siRNA (#1 or #2) and after 48 hrs, they were treated with 100 μM mito-TEMPO or vehicle (24 hrs). Then, they were analysed by FACS. Bars represents the SD of 3 independent experiments (n = 3).

Discussion

In this study, we clearly demonstrate that MAPK15 is a key player in cellular events contributing to the homeostasis of the mitochondrial compartment. Specifically, we show that this MAP kinase stringently regulates the mitophagic process from its very initial phases, when autophagosomes first interact with mitochondria. Still, our data also suggest that MAPK15 might control mitochondrial dynamics, possibly participating to mechanisms that segregates damaged organelles in the perinuclear area [42, 43], therefore not limiting its role only to speed up the mitophagic process, but also coordinating it to eventually spare intact mitochondria. Importantly, we show that MAPK15's role in mitophagy has also important biological implications, as a reduction of its expression induced an increase in the amount of mt-ROS which, in turn, caused extensive DNA damage, increased cellular senescence and reduced cell proliferation of knocked-down cells. Along this line, a recent demonstration that MAPK15 may affect chronic obstructive pulmonary disease (COPD) possibly by acting on the mitophagic process [12], supports our data and warrants further investigations.

As generation of ROS is a byproduct of cell growth, upon transformation cells sustain a much higher level of ROS production compared to normal cells [53]. Therefore, to avoid the damaging effects of oxidative stress, it is believed that cancer cells must actively up-regulate multiple antioxidant systems. Among them, autophagy contributes to clear cells of all irreversibly oxidized biomolecules and damaged mitochondria, therefore representing a fine mechanism to eliminate both the consequences and the source of oxidative stress, ultimately protecting cancer cells from oxidative damage [54]. It is, indeed, believed that cancer cells strongly depend on these mechanisms for survival, and that their inhibition may represent a potential therapeutic approach to take advantage of specific tumor vulnerabilities [55]. In this context, we have already shown both *in vitro* and *in vivo* that overexpression of MAPK15 gives a proliferative advantage to cancer cells [19, 26]. It is, therefore, tempting to speculate that this effect may be attributable, at least in part, to its ability to counteract endogenous oxidative stress and, possibly, oncogene-induced senescence [16]. Still, MAPK15 has also been involved in the response to other stressful stimuli, e.g., the shortage of nutrients which also often limits cancer growth and, therefore, more specific cancer models and approaches will be necessary to properly dissect MAPK15 functions relevant to this disease. Moreover, our

observation that, in different cell types, the mito-TEMPO mitochondria-targeted antioxidant strongly reduces nuclear damage provoked by MAPK15 down-regulation implies a strong contribution of mt-ROS to determine the mutagenic load of the cells. Still, we must emphasize that MAPK15 has been already involved also in other mechanisms controlling DNA damage. Among them, it is interesting to notice that this MAP kinase sustains the activity of TERT/Telomerase [20] an enzyme deeply involved in DDR and in opposing cellular senescence [16], again pointing to this MAP kinase as a key regulator of DNA damage, by controlling multiple proteins contributing to this process. Nonetheless, it is important to underline that even in the absence of exogenous chemical or physical insults, MAPK15 down-regulation is sufficient to determine a strong increase in nuclear DNA damage, supporting a key role for this kinase in the "housekeeping" control of the most dangerous source of mutagenic agents inside the cells, represented by old and damaged mitochondria eventually leading to chronic DNA damage, a leading cause of cellular senescence [16].

Eukaryotic cells are constantly subjected to changes of their micro-environmental conditions. Based on this, they continuously need to adapt to such changes to optimize their survival strategies. A key role in the response to such potentially harmful situations is based on the concerted action of different cell response pathways whose role is either to allow cells to adapt to novel external conditions or to commit cells to suicidal mechanisms, when excessively damaged. Data from our as well as from other laboratories now indicate MAPK15 as an important regulator of different adaptive response pathways, often interconnected among each other's, suggesting a potential major role for MAPK15 in integrating responses to such stimuli, which often determine important human pathologies. Importantly, dysfunctions in the mitophagic process have been linked to many pathological conditions, often related to aging, with neurodegenerative diseases probably representing the best examples [9]. Indeed, different proteins involved in mitophagy have been found mutated in PD (e.g., PINK1, LRRK2 and PRKN) and accumulation of α-synuclein may lead to mitochondrial dysfunctions and oxidative stress, ultimately resulting in neuronal cell death [56]. Of paramount interest, cellular senescence of astrocytes has been recently demonstrated to contribute to neurodegeneration in sporadic PD [57] and PD-causing pathogenetic mutations induces senescence in SH-SY5Y cells [58]. Intriguingly, *in vivo* depletion of senescent cells in a PD mouse model also determined a reduction in the development of

corresponding neurodegeneration [57], suggesting that strategies aimed at reducing an already established senescence phenotype may represent a successful approach to cure PD affected individuals. Overall, our current demonstration of the role of MAPK15 in supporting mitochondrial fitness in neuronal and non-neuronal cell lines therefore suggests that approaches targeting this kinase may allow the modulation of cell senescence in humans, to reduce its detrimental effects in PD and other age-related disorders or, alternatively, to increase its beneficial effects in aggressive neoplastic diseases.

Materials and Methods

Expression vectors

pCEFL-HA-MAPK15 and all its mutants were already described [13, 59]. pCEFL-MAPK15_WT IRES-GFP and all its mutants (AXXA; KD) were also previously described [26]. pRK5-Myc-Parkin (MYC-PRKN) (Addgene #17612) [60] and mCherry-parkin (mCherry-PRKN) (Addgene #23956) [10], were provided by Addgene as the kind gifts from the producing laboratories. The pDsRed2-Mito plasmid was purchased from Clontech (Cat. #63242).

Cell culture and transfections

SH-SY5Y cells were maintained in Dulbecco's modified Eagle medium (DMEM) F12 supplemented with 10% fetal bovine serum (FBS), 2 mM L-glutamine and 100 units/ml penicillin-streptomycin at 37°C in an atmosphere of 5% CO_2/air. HeLa cells were maintained in Dulbecco's modified Eagle medium (DMEM) supplemented with 10% fetal bovine serum (FBS), 2 mM L-glutamine and 100 units/ml penicillin-streptomycin at 37°C in an atmosphere of 5% CO_2/air. HeLa Empty vector IRES-GFP, HA-MAPK15_WT IRES-GFP, HeLa HA-MAPK15_KD IRES-GFP, HA-MAPK15_AXXA IRES-GFP and HeLa pDsRed2-Mito were generated by transfecting HeLa cells with corresponding plasmids and then subjected to selection with 2 mg/ml G-418. Western blot for overexpression experiments, 3×10^5 cells were seeded in 6-well cell culture plates and transfected with 1 μg of each expression vector using Lipofectamine LTX (Life Technologies, Monza, Italy), according to manufacturer's instructions. For western blot with interference experiments, 1×10^5 cells were seeded in 6-well cell culture plates, transfected with 100 nM of each SiRNA with Hiperfect (Qiagen), according to the manufacturer's instructions, then cells were harvested after 72hrs. The co-overexpression with pRK5-Myc-PRKN or mCherry-PRKN were performed 24 hrs after siRNA transfection using Lipofectamine LTX (Life Technologies, Monza, Italy). For confocal microscopy experiments, 5×10^4 cells were seeded on coverslips placed onto 12-well plates. Each sample was transfected with 200 ng of each plasmid using Lipofectamine LTX and then, 1×10^5 cells were seeded in 6-well cell culture plates for confocal microscopy experiments and transfected with 100 nM (HeLa cells) or 200 nM (SH-SY5Y cells) of each siRNA with Hiperfect (Qiagen), according to the

manufacturer's instructions. Twenty-four hours after transfection with siRNA, cells were transfected with mCherry-PRKN, where indicated, using Lipofectamine LTX (Life Technologies, Monza, Italy), according to manufacturer's instructions. Forty-eight hours after transfection with siRNA, cells were trypsinized and seeded on coverslips placed onto 12-well cell culture plates at the concentration of 5×10^4 cells/well. Fixation and staining with specific antibodies were performed 72 hrs after transfection.

Knock down of endogenous MAPK15

MAPK15-specific siRNA #1 (MAPK15 #1; target sequence 5'-TTGCTTGGAGGCTACTCCCAA-3') and control non-silencing siRNA (Scramble, target sequence 5'-AATTCTCCGAACGTGTCACGT-3') were obtained from Qiagen. MAPK15-specific siRNA #2 (MAPK15 #2; target sequence 5'-GACAGAUGCCCAGAGAACATT -3') was obtained from Eurofins Genomics. All siRNAs were transfected at a final concentration of 100 nM (HeLa) or 200 nM (SH-SY5Y) using Hiperfect (Qiagen). Samples were collected 72 hrs after transfection.

Reagents and antibodies

Bafilomycin A1 (Alfa Aesar) was used at final concentration of 100 nM; Hoechst 33342 and 4',6–Diamidino-2-fenilindolo diidrocloruro (DAPI) (from VWR) were used at final concentration of 0.01 mg/mL and 3 μM respectively; Carbonylcyanide-4-(trifluoromethoxy)-phenylhydrazone (FCCP) (Enzo Life Sciences) was used at final concentration of 30 μM. MitoSOX™ Red Mitochondrial Superoxide Indicator, for live-cell imaging (Thermo Fisher Scientific); 2-(N-(7-Nitrobenz-2-oxa-1,3-diazol-4-yl)Amino)-2-Deoxyglucose (2-NBDG) (Thermo Fisher Scientific); (2-(2,2,6,6-Tetramethylpiperidin-1-oxyl-4-ylamino)-2-oxoethyl)triphenylphosphonium chloride (Mito-TEMPO) (Sigma Aldrich); CellEvent Senescence Green Flow Cytometry Assay Kit (Thermo Fisher Scientific); DMEM, no glucose, no glutamine, no phenol red (Thermo Fisher Scientific). Seahorse XF Cell Mito Stress Test Kit, Glycolysis Stress Test Kit and Real-Time ATP Rate Assay Kit were purchased from Agilent Technologies. The following primary antibodies were used for western blots, confocal microscopy experiments: anti-MAPK15/ERK8 (custom preparation), anti-HA (Covance, MMS-101R) anti-LC3B (Nanotools, 0231-1000), anti-LC3B (MBL, M152-3), anti-MAPK1/ERK2 (Santa Cruz Biotechnology, sc-154), anti-LAMP1 (Santa Cruz

Biotechnology, sc-20011), Total OXPHOS Rodent WB Antibody Cocktail (abcam ab110413), anti-Tomm20 (F-10) (Santa Cruz Biotechnology, sc-17764), anti-COX IV (4D11-B3-E8) (Cell Signaling, mAb11967), γH2A.X (Cell Signaling, mAb9718). The following secondary antibodies were used for western blot experiments: anti-mouse (Santa Cruz Biotechnology, sc-2004) and anti-rabbit (Santa Cruz Biotechnology, sc-2005) HRP-conjugated IgGs.

Western blots

Total lysates were obtained by resuspending cellular pellets in RIPA buffer (50 mM TRIS-HCl pH 8.0, 150 mM NaCl, 0.5% sodium deoxycholate, 0.1% SDS, 1% NP-40) with the addition of protease inhibitors (cOmplete Protease Inhibitor cocktail, EDTA-free; Roche Diagnostics, Monza, Italy) and phosphatase inhibitors (2 mM NaF, 2 mM Na_3VO_4; Sigma Aldrich). Total proteins were quantified by Bradford assay and the same quantity of lysates was used for western blot analysis. Laemmli Loading Buffer 5X (250 mM Tris-HCl pH 6.8, 10% SDS, 50% glycerol, bromophenol blue) was added to protein samples, which were then heated for 5 min at 95°C or 50°C for when using Total OXPHOS Rodent WB Antibody Cocktail. Lysates were loaded on SDS-PAGE poly-acrylamide gel, transferred to Immobilon-P PVDF membrane (Merck Millipore), probed with appropriate antibodies, and revealed by enhanced chemiluminescence detection (ECL Plus; GE Healthcare, Milan, Italy). Densitometric analysis of western blots was performed with NIH Image J (National Institutes of Health).

Immunofluorescence

Cells were washed with PBS, fixed with ice-cold methanol for 10 min, and incubated with γH2A.X specific primary antibody for 1 hr. Alternatively, they were fixed with 4% paraformaldehyde in PBS for 20 min and permeabilized with 0.2% Triton X-100 solution for 5 min or 100 μg/ml digitonin solution (Invitrogen, BN2006) for 20 min for visualizing LC3B, then 20 min with 1% BSA in PBS. After blocking, cells were incubated with appropriate primary antibodies for 1 hr, washed three times with PBS, and then incubated with appropriate Alexa Fluor 488-conjugated (Invitrogen, A21202) or Alexa Fluor 647-conjugated (Invitrogen, A21245) secondary antibodies and then washed again three times in PBS. Nuclei were stained with 1.5 μM 4′,6-diamidino-2-

phenylindole (DAPI) in PBS for 5 min. Coverslips were mounted in fluorescence mounting medium (Dako, S3023). Samples were visualized on a TSC SP5 confocal microscope (Leica, 5100000750) installed on an inverted LEICA DMI 6000CS (10741320) microscope using an oil immersion PlanApo 40× 1.25 NA objective or an oil immersion PlanApo 63× 1.4 NA objective. Images were acquired using the LAS AF acquisition software (Leica Microsystems).

Mitochondrial DNA copy number quantitation and analysis of gene expression

Total RNA was purified using QIAzol LysisReagent (Qiagen). Reverse transcription was performed with the QuantiTect Reverse Transcription Kit (Qiagen). Total DNA was purified using QIAamp DNA Mini Kit and loaded 10 ng of purified DNA on each RT-PCR reaction. RT-PCR was performed with Luna Universal qPCR Master Mix on a Rotor-Gene 6000 RT-PCR system (Corbett Life Science). The following primer pairs were used:

MT-ND1 FW 5'-GGCTATATACAACTACGCAAAGGC-3';

MT-ND1 RV 5'-GGTAGATGTGGCGGGTTTTAGG-3';

MT-ND2 FW 5'-CTTCTGAGTCCCAGAGGTTACC-3';

MT-ND2 RV 5'-GAGAGTGAGGAGAAGGCTTACG-3';

PKM FW 5'-ATGGCTGACACATTCCTGGAGC-3';

PKM RV 5'-CCTTCAACGTCTCCACTGATCG-3';

MAPK15 FW 5'-TGGCCAGCGTACAACAGGT-3';

MAPK15 RV 5'-CAGTCCCGTAGGCTTGGGAGTA-3';

MAPK1 FW 5'-GCCCATCTTTCCAGGGAAGCATTA-3';

MAPK1 RV 5'-AGAGCTTTGGAGTCAGCATTTGGG-3'.

Mitochondrial ROS production

The MitoSOX™ Red fluorescent probe (Molecular Probes, Inc., Eugene, OR, USA) is able to accumulate in mitochondria due to their positive charge, and its oxidation by

superoxide produces red fluorescence that can be easily measured [61]. To quantify mitochondrial ROS production we incubated, 5 μM of MitoSOX with cells in full medium for 10 minutes, according to the manufacturer's protocol. Samples were acquired on a FACSCanto II flow cytometer (BD Biosciences). Data were analyzed with FlowJo software. All analyses were performed in triplicate.

Mitochondrial enrichment

Cells were homogenized in RLM buffer (250 mM sucrose, 10 mM Tris–HCl [pH 7.5], 0,1 mM EGTA, 1 mM dithiothreitol, 2mM Na_3VO_4, 2 mM NaF) with the addition of protease inhibitors. Homogenates were centrifuged at 1000×g for 10 min at 4°C, the pellet were used as total fraction and the supernatant were collected and centrifuged at 6000×g for 10 min at 4°C. The supernatant was designated the cytosolic fraction, and the pellet was used as the mitochondrial enriched fraction. The pellets were resuspended in lysis buffer (20 mM HEPES, pH=7.5, 10 mM EGTA, 40 mM β-glycerophosphate, 1% NP-40, 2.5 mM $MgCl_2$, 2 mM orthovanadate, 2 mM NaF, 1 mM DTT, Roche protease inhibitors cocktail). Then, samples were subjected to protein quantification and western blot analysis.

Seahorse Analysis

Cells were seeded in XFe96 cell culture plates with 2×10^4 cells per well and after 24h subjected to the extracellular flux (XF). For the XF glycolysis stress test, XF assay medium was supplemented with 2 mM glutamine and incubated at 37 °C in a non-CO_2 incubator for 1 hr before the analysis. This analysis is performed in real-time by measuring ECAR and OCR after Glucose (10mM) oligomycin (1.5 μM) and 2-DG (50 mM) administration. For the XF Mito Stress test and Real-Time ATP Rate XF base medium were supplemented with 10 mM glucose, 2 mM glutamine and 1 mM sodium pyruvate. Cells were incubated for 1h at 37 °C in a non-CO_2 incubator before the analysis. This analysis is performed by real-time measurement of ECAR and OCR after a sequence of compounds, for the Mito Stress test oligomycin were used (1.5 μM), carbonyl cyanide-4 (trifluoromethoxy) phenylhydrazone (FCCP) (1 μM) and Rotenone/Antimycin A (0.5 μM). For the XF Real-Time ATP Rate were used oligomycin (1.5 μM) and Rotenone/Antimycin A (0.5 μM). Protein quantification was used to normalize the results. Results were analyzed using Wave 2.6 desktop software.

β-galactosidase activity

Senescence was monitored with fluorescence-based detection of β-galactosidase activity using the CellEvent Senescence Green Flow Cytometry Assay kit. HeLa cell line were subjected to siRNA transfection to knock down endogenous MAPK15 and after 24h, we overexpressed MYC-PRKN. Alternatively, we downregulated MAPK15 in SH-SY5Y, and 48 hrs after, cells were treated with mito-TEMPO (100 μM), where indicated, for 24 hrs. After 72 hrs of siRNA transfection, we fixed cells in 4% paraformaldehyde in PBS for 20 min. Then samples, were incubated with CellEvent Senescence Green Probe at 37°C for 2 hours in the absence of CO_2 following manufacturer's instructions (Thermo Fisher Scientific). Samples were subjected to flow cytometer analysis, acquired with FACSCanto II cytometer (BD Biosciences).

2-NDBG Glucose Uptake

Cells (2 x10^4) were seeded in 96-well plate and, after 24 hrs, cells were washed with PBS, and incubated with glucose and FBS free medium containing 0.02 mg/mL of 2-NDBG for 1hr at 37°C and 5%CO_2/air. After incubation, we washed cells with PBS and detected fluorescence with SpectroMax M2 microplate reader (Molecular Devices). Each well fluorescence was normalized by protein quantitation.

Cells proliferation

Cells (1×10^5) were seeded in 6-well plates, then subjected to siRNA transfection. After 48 hrs, cells were treated with vehicle or mito-TEMPO (100 μM) for 24 hrs. After 72 hrs from transfection, cell number were evaluated using Z2 Coulter Counter (Beckman Coulter).

Statistical analysis

LC3B-dots count, mitochondrial in acidic condition, mitochondrial volume and fluorescence intensity were analyzed using the Quantitation Module of Volocity software (PerkinElmer Life Science, I40250). Significance (p value) was assessed by Student's t test, using GraphPad Prism8 software. Asterisks were attributed as follows: *$p<0.05$, **$p<0.01$, ***$p<0.001$.

References

[1] Galluzzi L, Kepp O, Trojel-Hansen C et al. Mitochondrial control of cellular life, stress, and death. Circ Res. 2012; 111:1198-1207.

[2] Suomalainen A, Battersby BJ. Mitochondrial diseases: the contribution of organelle stress responses to pathology. Nat Rev Mol Cell Biol. 2018; 19:77-92.

[3] Chance B, Sies H, Boveris A. Hydroperoxide metabolism in mammalian organs. Physiol Rev. 1979; 59:527-605.

[4] Kirkinezos IG, Moraes CT. Reactive oxygen species and mitochondrial diseases. Semin Cell Dev Biol. 2001; 12:449-457.

[5] Campisi J. Aging, cellular senescence, and cancer. Annu Rev Physiol. 2013; 75:685-705.

[6] Fernandez-Marcos PJ, Serrano M. Mitochondrial Damage Induces Senescence with a Twisted Arm. Cell Metab. 2016; 23:229-230.

[7] Sun N, Youle RJ, Finkel T. The Mitochondrial Basis of Aging. Mol Cell. 2016; 61:654-666.

[8] Zachari M, Ktistakis NT. Mammalian Mitophagosome Formation: A Focus on the Early Signals and Steps. Front Cell Dev Biol. 2020; 8:171.

[9] Yoo SM, Jung YK. A Molecular Approach to Mitophagy and Mitochondrial Dynamics. Mol Cells. 2018; 41:18-26.

[10] Narendra D, Tanaka A, Suen DF et al. Parkin is recruited selectively to impaired mitochondria and promotes their autophagy. J Cell Biol. 2008; 183:795-803.

[11] Lau ATY, Xu YM. Regulation of human mitogen-activated protein kinase 15 (extracellular signal-regulated kinase 7/8) and its functions: A recent update. J Cell Physiol. 2018; 234:75-88.

[12] Zhang M, Fang L, Zhou L et al. MAPK15-ULK1 signaling regulates mitophagy of airway epithelial cell in chronic obstructive pulmonary disease. Free Radic Biol Med. 2021; 172:541-549.

[13] Colecchia D, Strambi A, Sanzone S et al. MAPK15/ERK8 stimulates autophagy by interacting with LC3 and GABARAP proteins. Autophagy. 2012; 8:1724-1740.

[14] Colecchia D, Dapporto F, Tronnolone S et al. MAPK15 is part of the ULK complex and controls its activity to regulate early phases of the autophagic process. J Biol Chem. 2018; 293:15962-15976.

[15] Zacharogianni M, Kondylis V, Tang Y et al. ERK7 is a negative regulator of protein secretion in response to amino-acid starvation by modulating Sec16 membrane association. EMBO J. 2011; 30:3684-3700.

[16] Di Micco R, Krizhanovsky V, Baker D et al. Cellular senescence in ageing: from mechanisms to therapeutic opportunities. Nat Rev Mol Cell Biol. 2021; 22:75-95.

[17] Klevernic IV, Martin NM, Cohen P. Regulation of the activity and expression of ERK8 by DNA damage. FEBS Lett. 2009; 583:680-684.

[18] Li Z, Li N, Shen L et al. Quantitative Proteomic Analysis Identifies MAPK15 as a Potential Regulator of Radioresistance in Nasopharyngeal Carcinoma Cells. Front Oncol. 2018; 8:548.

[19] Rossi M, Colecchia D, Ilardi G et al. MAPK15 upregulation promotes cell proliferation and prevents DNA damage in male germ cell tumors. Oncotarget. 2016; 7:20981-20998.

[20] Cerone MA, Burgess DJ, Naceur-Lombardelli C et al. High-throughput RNAi screening reveals novel regulators of telomerase. Cancer Res. 2011; 71:3328-3340.

[21] Groehler AL, Lannigan DA. A chromatin-bound kinase, ERK8, protects genomic integrity by inhibiting HDM2-mediated degradation of the DNA clamp PCNA. J Cell Biol. 2010; 190:575-586.

[22] Mizumura K, Cloonan SM, Nakahira K et al. Mitophagy-dependent necroptosis contributes to the pathogenesis of COPD. J Clin Invest. 2014; 124:3987-4003.

[23] Kausar S, Wang F, Cui H. The Role of Mitochondria in Reactive Oxygen Species Generation and Its Implications for Neurodegenerative Diseases. Cells. 2018; 7

[24] Redmann M, Benavides GA, Wani WY et al. Methods for assessing mitochondrial quality control mechanisms and cellular consequences in cell culture. Redox Biol. 2018; 17:59-69.

[25] Strappazzon F, Nazio F, Corrado M et al. AMBRA1 is able to induce mitophagy via LC3 binding, regardless of PARKIN and p62/SQSTM1. Cell Death Differ. 2015; 22:419-432.

[26] Colecchia D, Rossi M, Sasdelli F et al. MAPK15 mediates BCR-ABL1-induced autophagy and regulates oncogene-dependent cell proliferation and tumor formation. Autophagy. 2015; 11:1790-1802.

[27] TeSlaa T, Teitell MA. Techniques to monitor glycolysis. Methods Enzymol. 2014; 542:91-114.

[28] Nitin N, Carlson AL, Muldoon T et al. Molecular imaging of glucose uptake in oral neoplasia following topical application of fluorescently labeled deoxy-glucose. Int J Cancer. 2009; 124:2634-2642.

[29] Yamada K, Saito M, Matsuoka H et al. A real-time method of imaging glucose uptake in single, living mammalian cells. Nat Protoc. 2007; 2:753-762.

[30] Li N, Ragheb K, Lawler G et al. Mitochondrial complex I inhibitor rotenone induces apoptosis through enhancing mitochondrial reactive oxygen species production. J Biol Chem. 2003; 278:8516-8525.

[31] Slepchenko KG, Lu Q, Li YV. Cross talk between increased intracellular zinc (Zn^{2+}) and accumulation of reactive oxygen species in chemical ischemia. Am J Physiol Cell Physiol. 2017; 313:C448-C459.

[32] Klionsky DJ, Abdel-Aziz AK, Abdelfatah S et al. Guidelines for the use and interpretation of assays for monitoring autophagy (4th edition)[1]. Autophagy. 2021; 17:1-382.

[33] Boya P, González-Polo RA, Casares N et al. Inhibition of macroautophagy triggers apoptosis. Mol Cell Biol. 2005; 25:1025-1040.

[34] Wong YC, Ysselstein D, Krainc D. Mitochondria-lysosome contacts regulate mitochondrial fission via RAB7 GTP hydrolysis. Nature. 2018; 554:382-386.

[35] Zhou Y, Long Q, Wu H et al. Topology-dependent, bifurcated mitochondrial quality control under starvation. Autophagy. 2020; 16:562-574.

[36] Tan VP, Smith JM, Tu M et al. Dissociation of mitochondrial HK-II elicits mitophagy and confers cardioprotection against ischemia. Cell Death Dis. 2019; 10:730.

[37] Gao F, Zhang Y, Hou X et al. Dependence of PINK1 accumulation on mitochondrial redox system. Aging Cell. 2020; 19:e13211.

[38] Zhang W, Ma Q, Siraj S et al. Nix-mediated mitophagy regulates platelet activation and life span. Blood Adv. 2019; 3:2342-2354.

[39] Chan NC, Salazar AM, Pham AH et al. Broad activation of the ubiquitin-proteasome system by Parkin is critical for mitophagy. Hum Mol Genet. 2011; 20:1726-1737.

[40] Geisler S, Holmström KM, Skujat D et al. PINK1/Parkin-mediated mitophagy is dependent on VDAC1 and p62/SQSTM1. Nat Cell Biol. 2010; 12:119-131.

[41] Monzio Compagnoni G, Kleiner G, Bordoni A et al. Mitochondrial dysfunction in fibroblasts of Multiple System Atrophy. Biochim Biophys Acta Mol Basis Dis. 2018; 1864:3588-3597.

[42] Okatsu K, Saisho K, Shimanuki M et al. p62/SQSTM1 cooperates with Parkin for perinuclear clustering of depolarized mitochondria. Genes Cells. 2010; 15:887-900.

[43] Vives-Bauza C, Zhou C, Huang Y et al. PINK1-dependent recruitment of Parkin to mitochondria in mitophagy. Proc Natl Acad Sci U S A. 2010; 107:378-383.

[44] Lu X, Zhang Y, Bai H et al. Mitochondria-targeted antioxidant MitoTEMPO improves the post-thaw sperm quality. Cryobiology. 2018; 80:26-29.

[45] Porporato PE, Payen VL, Pérez-Escuredo J et al. A mitochondrial switch promotes tumor metastasis. Cell Rep. 2014; 8:754-766.

[46] Correia-Melo C, Marques FD, Anderson R et al. Mitochondria are required for pro-ageing features of the senescent phenotype. EMBO J. 2016; 35:724-742.

[47] Herranz N, Gil J. Mitochondria and senescence: new actors for an old play. EMBO J. 2016; 35:701-702.

[48] García-Prat L, Martínez-Vicente M, Perdiguero E et al. Autophagy maintains stemness by preventing senescence. Nature. 2016; 529:37-42.

[49] Dimri GP, Lee X, Basile G et al. A biomarker that identifies senescent human cells in culture and in aging skin in vivo. Proc Natl Acad Sci U S A. 1995; 92:9363-9367.

[50] Puspita L, Chung SY, Shim JW. Oxidative stress and cellular pathologies in Parkinson's disease. Mol Brain. 2017; 10:53.

[51] Di Rita A, D'Acunzo P, Simula L et al. AMBRA1-Mediated Mitophagy Counteracts Oxidative Stress and Apoptosis Induced by Neurotoxicity in Human Neuroblastoma SH-SY5Y Cells. Front Cell Neurosci. 2018; 12:92.

[52] Van Humbeeck C, Cornelissen T, Hofkens H et al. Parkin interacts with Ambra1 to induce mitophagy. J Neurosci. 2011; 31:10249-10261.

[53] Trachootham D, Zhou Y, Zhang H et al. Selective killing of oncogenically transformed cells through a ROS-mediated mechanism by beta-phenylethyl isothiocyanate. Cancer Cell. 2006; 10:241-252.

[54] Filomeni G, De Zio D, Cecconi F. Oxidative stress and autophagy: the clash between damage and metabolic needs. Cell Death Differ. 2015; 22:377-388.

[55] Luo J, Solimini NL, Elledge SJ. Principles of cancer therapy: oncogene and non-oncogene addiction. Cell. 2009; 136:823-837.

[56] Gao F, Yang J, Wang D et al. Mitophagy in Parkinson's Disease: Pathogenic and Therapeutic Implications. Front Neurol. 2017; 8:527.

[57] Chinta SJ, Woods G, Demaria M et al. Cellular Senescence Is Induced by the Environmental Neurotoxin Paraquat and Contributes to Neuropathology Linked to Parkinson's Disease. Cell Rep. 2018; 22:930-940.

[58] Ho DH, Seol W, Son I. Upregulation of the p53-p21 pathway by G2019S LRRK2 contributes to the cellular senescence and accumulation of α-synuclein. Cell Cycle. 2019; 18:467-475.

[59] Iavarone C, Acunzo M, Carlomagno F et al. Activation of the Erk8 mitogen-activated protein (MAP) kinase by RET/PTC3, a constitutively active form of the RET proto-oncogene. J Biol Chem. 2006; 281:10567-10576.

[60] Zhang Y, Gao J, Chung KK et al. Parkin functions as an E2-dependent ubiquitin-protein ligase and promotes the degradation of the synaptic vesicle-associated protein, CDCrel-1. Proc Natl Acad Sci U S A. 2000; 97:13354-13359.

[61] Kauffman ME, Kauffman MK, Traore K et al. MitoSOX-Based Flow Cytometry for Detecting Mitochondrial ROS. React Oxyg Species (Apex). 2016; 2:361-370.